16p.

NASA TN D-1419

9

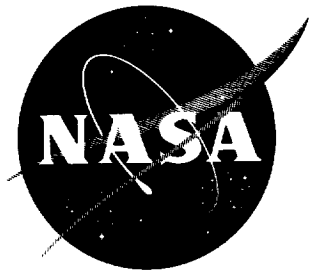

TECHNICAL NOTE

D-1419

A PHASE-LOCKED PHASE FILTER FOR THE MINITRACK SYSTEM

Ronald F. Woodman

Goddard Space Flight Center

NATIONAL AERONAUTICS AND SPACE ADMINISTRATION

WASHINGTON

September 1962

A PHASE-LOCKED PHASE FILTER FOR THE MINITRACK SYSTEM

by
Ronald F. Woodman
Goddard Space Flight Center

SUMMARY

A variable-bandwidth filter has been designed and built to narrow the postdetection bandwidth of the Minitrack satellite tracking system. It is based on phase-lock techniques. At its narrowest bandwidth, 0.03 cps, the phase peak-to-peak noise deviations are reduced to ±1.5 percent of a wavelength for a signal strength of -140 dbm coming into the receiver "front ends". The filter introduces no phase shift or time delay regardless of the signal phase rate.

CONTENTS

A PHASE-LOCKED PHASE FILTER FOR THE MINITRACK SYSTEM

by
Ronald F. Woodman*
Goddard Space Flight Center

INTRODUCTION

The Minitrack satellite tracking system has proven to be sensitive enough for normal satellite orbits with altitudes from a few hundred to a few thousand miles, but for satellites and space probes at altitudes higher than ten thousand miles the sensitivity is inadequate. Two possible solutions are to increase the power of the satellite beacon or increase the sensitivity of the tracking system. The former has technical and economical limitations, but a large increase of the tracking system sensitivity is a technically feasible and much less expensive solution.

The sensitivity of the Minitrack system is determined by the 10-cps postdetection bandwidth for signals above the IF detector threshold (-140 dbm). This 10 cps bandwidth is the bandwidth of the 100 cps filter between the phase meter and receiver. It was selected as the narrowest bandwidth to allow a signal with a differential doppler frequency of 1 cps (phase rate of approximately one wavelength per second) to go through the filter with a linear phase-versus-frequency correction. The differential doppler frequency or phase rate gets lower as the satellite orbit gets higher. This should allow a reduction of the postdetection bandwidth and compensate for the reduction of the received power. Unfortunately, it is very hard, if not impossible, to build 100-cps passive filters narrower than a few cps with the desired phase stability. Even with active filters, it is hard to get bandwidths narrower than 0.5 cps without having stability problems. The filter to be described here does not have the above limitations; bandwidths as narrow as desired can be achieved. Furthermore, it does not introduce any phase shift or time delay; thus it allows a narrower bandwidth for a particular phase rate. The bandwidth is limited only by the corresponding settling or acquisition time.

*Mr. Woodman is an employee of the Instituto Geofisico del Peru working for the Lima, Peru, Minitrack Station. He has been detailed to GSFC as part of an international cooperation program.

SYSTEM THEORY

Figure 1 is a block diagram of the system described in this report. The output of the 100-cps phase shifter is phase-locked to the phase of the 100-cps signal; the phase difference, if any, is amplified by an operational amplifier, with the proper frequency characteristics, which drives a servo amplifier. The servo motor drives the resolver phase shifter until the phase difference is reduced to zero. The output of the phase shifter, ϕ_p', is equal to the reference phase ϕ_r plus the angular rotation ϕ_p of the resolver motor. The phase ϕ_s' of the signal is equal to the reference phase ϕ_r plus the information phase ϕ_s. And since ϕ_p' equals ϕ_s' because of the servo loop, we can write:

$$\phi_p' = \phi_r + \phi_p = \phi_r + \phi_s = \phi_s' ,$$

or

$$\phi_p = \phi_s . \tag{1}$$

Therefore the angular rotation of the resolver is equal to the phase of the signal containing the information. This information can be picked up by means of a potentiometer or a digital encoder. Equation 1 holds only for a clear signal under steady-state conditions. For a ϕ_s that is varying, ϕ_p and ϕ_s are related by the system transfer function:

$$G(s) = \frac{\phi_p(s)}{\phi_s(s) - \phi_p(s)} ,$$

where s is the Laplacian operator, or by

$$\frac{\phi_p(s)}{\phi_s(s)} = \frac{G(s)}{1 + G(s)} . \tag{2}$$

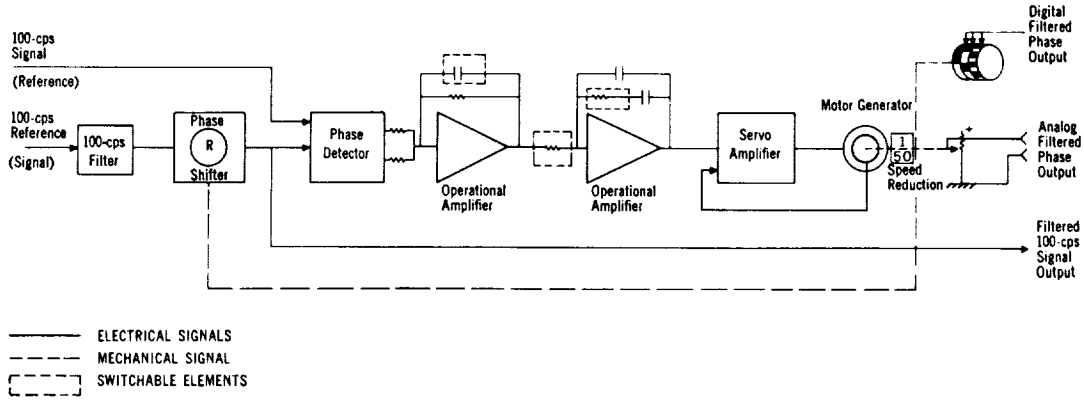

Figure 1—Phase-locked Phase Filter Block Diagram

The system can work in two different modes (Figure 1): one as described, in which the 100-cps reference is fed to the phase shifter and kept in phase with the 100-cps signal, and the other mode in which the 100-cps signal is shifted and kept in phase with the reference. Equations 1 and 2 hold for both modes of operation, but each mode has an advantage lacking in the other. The advantage of the first is that the filtered information can be picked up either from the resolver shaft rotation with a potentiometer or from the phase of the clean 100-cps output of the phase shifter by feeding it into the existing analog and digital Minitrack phase meters. The advantage of the second mode is that the frequency of the signal after it goes through the resolver is always 100-cps and in phase with the reference. This permits the use of the existing 100-cps Minitrack filter between the phase shifter and the detector to produce a narrower bandwidth without introducing phase shift. A narrower 100-cps filter bandwidth would also improve the threshold of the phase detector.

In either case, the signal is used as the square wave from the limiting stages of the Minitrack phase meter in order to take advantage of the quieting effects of this limiting and to get rid of the amplitude variations. It is filtered back to sinusoidal if it goes to the shifter, or left as a square wave if it goes directly to the detector.

The system's adjustable transfer function, $G(s)$, gives the different frequency characteristics and the desired filtering action. There are three different frequency characteristics, under the control of a switch, which give three different bandwidths: approximately 3, 0.3, and 0.03 cps. Figure 2 shows a normalized linear approximation of the open loop frequency characteristics of the system which holds for the different bandwidths with the corresponding value of the frequency ω.

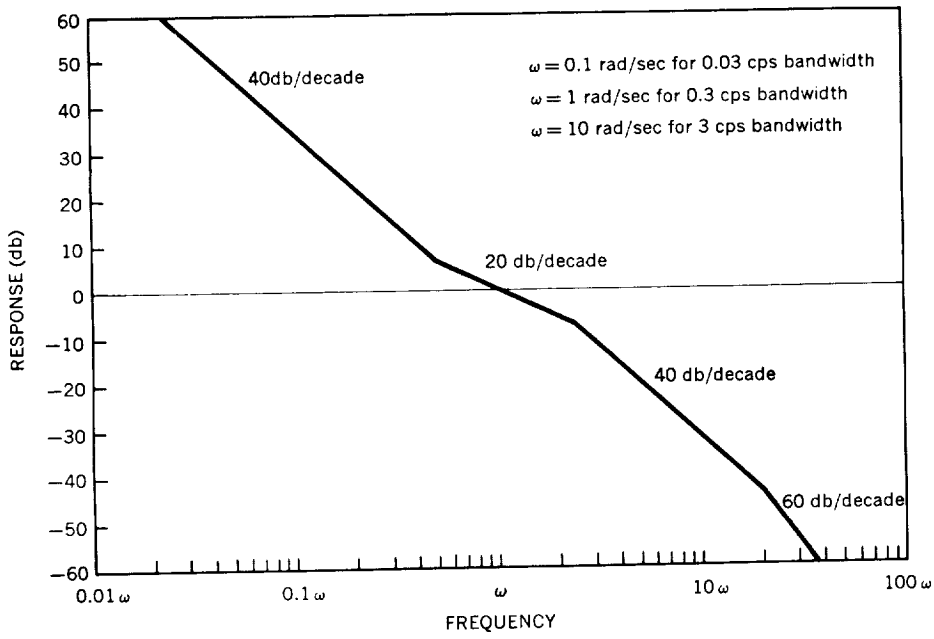

Figure 2—Normalized open-loop frequency response of the system

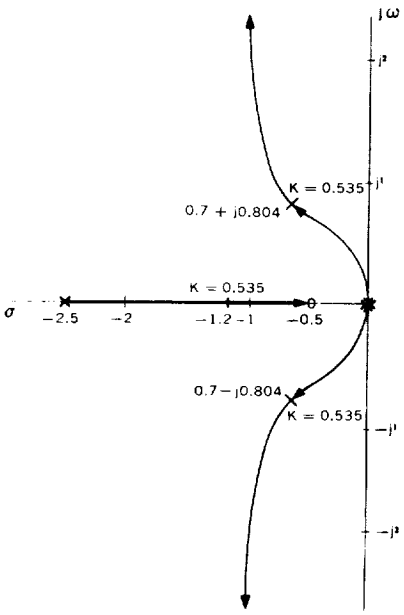

Figure 3—Root loci of the closed loop

The 40 db/decade at the low frequency end is accomplished by means of a double integration: one integration is done by the 10 μf capacitor in the feedback of the operational amplifier, and the other by the velocity-controlled servo motor. It is because of this double integration that no phase shift or time delay is introduced despite the narrow bandwidth of the system. Just before the 40 db/decade line cuts the 0 db line there is a break to 20 db/decade for stability; then the line is broken back to 40 db/decade for a steeper roll-off.

The corresponding normalized open-loop transfer function is

$$G(s') = 5K' \frac{s' + 0.5}{s'^2(s' + 2.5)}, \qquad (3)$$

where $s' = 0.1\,s$, $1\,s$, or $10\,s$ for a 3, 0.3, or 0.03 cps bandwidth, respectively. Higher frequency poles have been dropped for simplicity. The pole and zero configuration of the open-loop transfer function and the locus of the closed loop poles for different gains are shown in Figure 3; a gain of $K' = 0.535$ has been chosen for maximum damping. The corresponding closed-loop transfer function is

$$\frac{\phi_r(s)}{\phi_s(s)} = 2.68 \frac{s' + 0.5}{(s' + 1.2)(s' + 0.7 + j\,0.804)(s' + 0.7 - j\,0.804)}$$

$$= 2.68 \frac{s' + 0.5}{(s' + 1.2)(s'^2 + 1.4s' + 1.13)}. \qquad (4)$$

The closed-loop frequency response derived from the above transfer function is plotted in Figure 4. The -3 db point occurs at $s' = 1.9$, which corresponds to 19, 1.9, and 0.19 radians/second or 3, 0.3, and 0.03 cps and to an improvement of 5, 15, and 25 db, respectively, over the signal-to-noise ratio with a 10-cps filter. A 25 db improvement should result in a reduction of the peak-to-peak deviations by a factor of 20; therefore, for a -140 dbm signal with a peak-to-peak phase deviation of ± 50 percent of a wavelength, the noise would be reduced to ± 2.5 percent of a wavelength. The actual system performs even better because of the reduction of noise peaks by the nonlinearity inherent in the phase detector.

It was mentioned that this system does not introduce any phase shift for a constant phase rate input regardless of the bandwidth. This is equivalent to stating that the

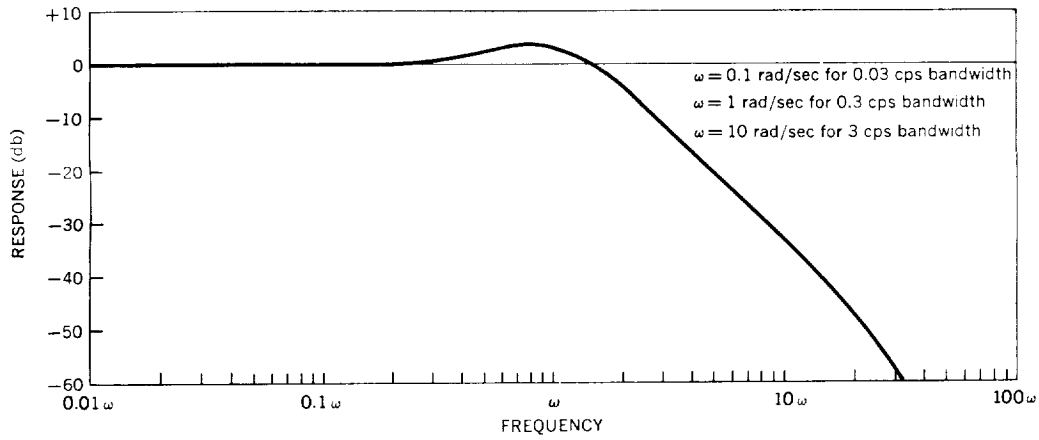

Figure 4—Normalized closed-loop frequency response

steady-state loop error is zero for a ramp input. The error-versus-input transfer function is

$$\frac{\phi_e(s')}{\phi_s(s')} = \frac{\phi_s(s') - \phi_r(s')}{\phi_s(s')} = \frac{1}{1 + G(s')}$$

$$= \frac{s'^2(s' + 2.5)}{(s' + 1.2)(s'^2 + 1.4s' + 1.13)} \quad . \tag{5}$$

For a ramp input of $1/s^2$,

$$\phi_e(s') = \frac{(s' + 2.5)}{(s' + 1.2)(s'^2 + 1.4s' + 1.13)} \quad . \tag{6}$$

In the time domain (normalized time)

$$\phi_e(t') = 1.53\left[e^{-1.2t'} - e^{-0.7t'}(\cos 0.804t' - 1.45 \sin 0.804t')\right] \quad , \tag{7}$$

where the error is reduced to zero when the value of t' is much larger than 1. The error function $\phi_e(t')$, as well as the response function for a unity ramp input, is shown in Figure 5. From either this graph or Equation 7, it can be determined that there is a settling time of the order of 8 t' to 10 t'. With no phase shift limitation, this transient time is the limiting factor in the use of a particular bandwidth for different phase rates.

The Minitrack fine antenna beam pattern is 10 degrees wide to the -6 db points (24 degrees wide from null to null) and a satellite takes approximately 10 times the inverse of its phase rate in degrees/second to cross it. With the system in the 0.03-cps mode,

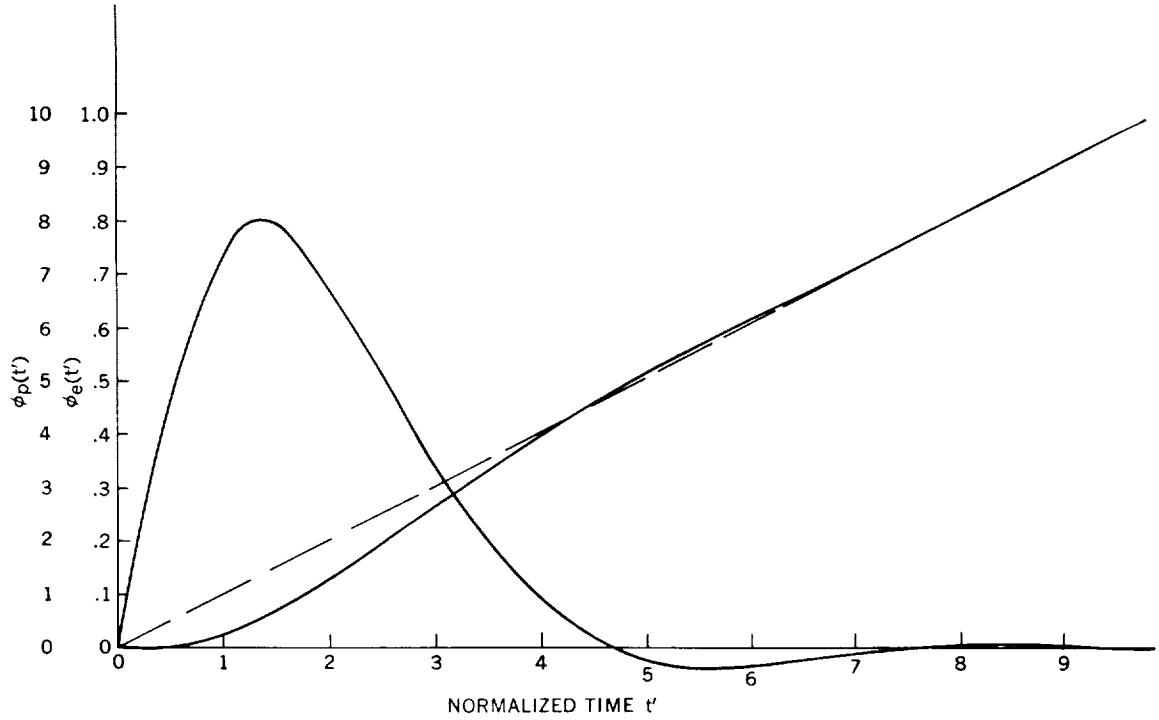

Figure 5—Ramp input response

it will take 80 seconds to acquire to within 0.1 percent of a wavelength (0.001 space degree) for a satellite phase rate of 0.05 degree/second. At this phase rate, it will take the satellite 200 seconds to cross the main beam, of which 80 seconds will be used for acquisition and the rest for useful information. If this bandwidth were used for satellite passes with a maximum phase rate of 0.05 degree/second, the bandwidth would take care of all passes with ranges of the order of 10,000 miles or higher. This bandwidth would be particularly useful in tracking radio stars for calibration purposes.

The 0.3 cps bandwidth will take 8 seconds to acquire a signal with a phase rate of 0.5 degree/second and at this phase rate the satellite will take 20 seconds to cross the main beam, 12 seconds of which will provide useful information. The phase rate of 0.5 degrees/second is about the maximum rate for normal satellite orbits, so the 0.3 cps bandwidth will take care of most of the passes in normal operation, with the corresponding improvement in sensitivity.

The few passes with phase rates faster than 0.5 degree/second will be taken care of by the 3 cps bandwidth with an 0.8 second acquisition time.

The settling time of the system for a step input is the same as the one for a ramp input. The error function for a unity step input is defined by

$$\phi_e(s') = \frac{s'(s' + 2.5)}{(s' + 1.2)(s'^2 + 1.4s' + 1.13)} , \quad (8)$$

or in the time domain by

$$\phi_e(t') = -e^{-1.2t'} + 2e^{-0.7t'}(\cos 0.804t' - 0.304 \sin 0.804) . \quad (9)$$

This has been plotted in Figure 6.

Another advantage of this system is the fact that the shaft rotation output is a continuous function of the phase of the input signal, as compared with the discontinuous sawtooth output of the phase measuring system in use. A continuous phase output makes it relatively easy to solve the Minitrack system ambiguity on the site on a real time basis. The Minitrack position information, free from ambiguity, could be used for different applications, such as in the plotting of satellite position and in the driving of telemetry antennas and optical cameras. A computer is being built which will solve the system ambiguity and plot the satellite position in real time.

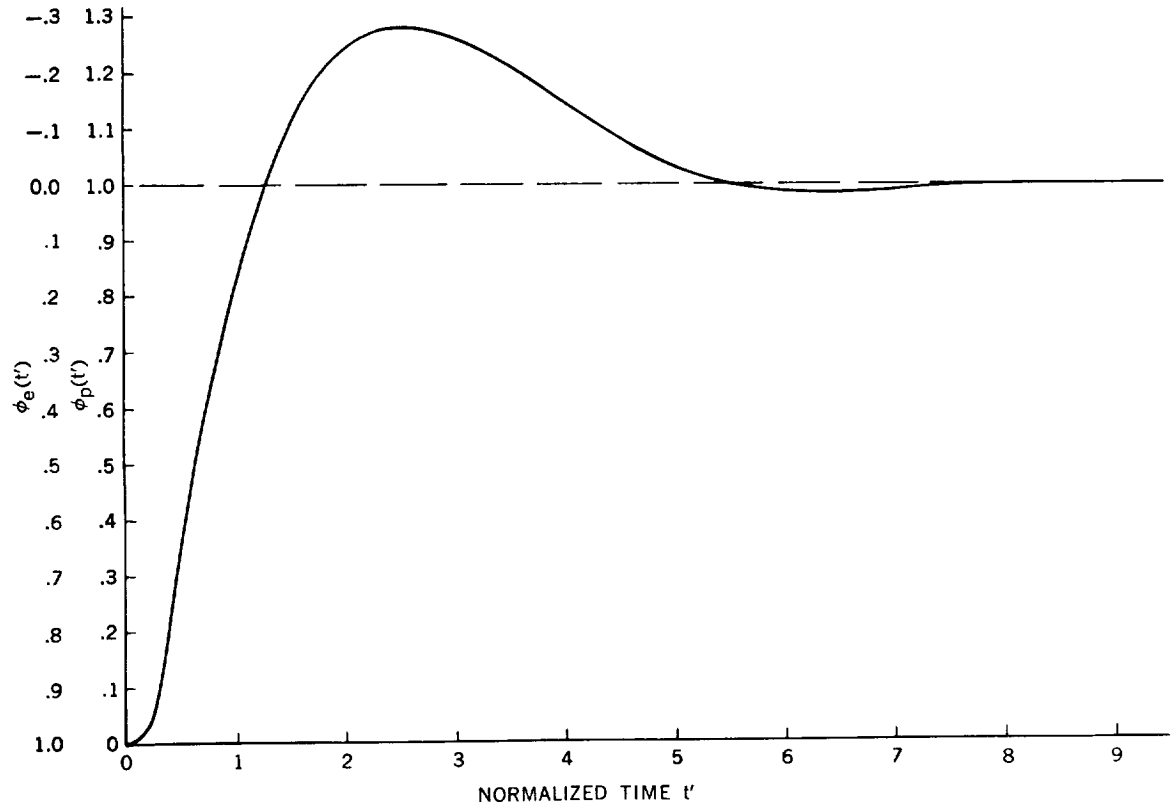

Figure 6—Step input response

PHYSICAL DESCRIPTION OF THE SYSTEM

The system consists of the following parts: A filter, a resolver phase shifter, a phase detector, an operational amplifier, a Brown servo amplifier driving a motor-generator, and a position potentiometer. The filter, phase shifter, detector, and operational amplifier are in one chassis (Figure 7). The filter is a standard LC 100-cps bandpass filter. Its function is to convert the square wave input into a sinusoid before it goes into the phase shifter. The phase shifting is done with a precision Reeves resolver. The accuracy of the whole system depends mainly on the linear relationship between the output phase and the shaft rotation. With the circuit used, this accuracy has been measured to be ± 0.001 revolution (± 0.1 percent of a wavelength).

The phase detector design is conventional. A large-value capacitor has been connected across the detecting diodes to improve the detector's efficiency and provide some high frequency noise filtering. The summing of the outputs is done by the operational amplifier. The operational amplifier consists of two Philbrick K2-W operational amplifiers connected in series. The first one is a summing and buffer amplifier for the phase detector; its bias adjustment is used to null its own bias and to cancel any unbalance from the phase detector. There is a switchable feedback capacitor to produce some high frequency filtering (places a pole at $s' = 25$), and to help in smoothing the 100-cps ripple from the phase detector. The second operational amplifier defines the important frequency characteristics of the system, performs one integration, controls the gain of the open loop and thus the bandwidth of the closed-loop system, and provides the proper stabilizing compensation for closed-loop stability. When changing from one bandwidth to another, only resistive elements are switched so that no transient will be produced. This allows the use of the 10 μf integrating capacitor to provide a memory of the system phase rate while the bandwidth is switched. There is a switch across the capacitor for quick discharge. Error voltages are kept higher than 5 volts/wavelength to minimize the effect of the dc amplifier drift.

The servo amplifier accepts dc error signals and has provision for velocity feedback. It drives the motor-generator; the generator is an integral unit with the motor and its output is fed back to the amplifier. Velocity feedback is necessary for damping purposes, and makes the effective time constant of the motor small enough that it does not affect the stability of the servo loop. With velocity feedback, there is a much higher torque-to-error ratio for a particular loop gain, thus minimizing the effects of mechanical friction and increasing the dynamic range of the system. There is a gear ratio of 50:1 between the motor and resolver—the largest ratio that allows the system to track 1 wavelength/second phase rates. Smaller ratios result in insufficient torque for the motor to overcome friction when working on the 0.03 cps bandwidth. With the 3 cps bandwidth, a 10:1 gear ratio is necessary to track 5 lobes/second phase rates and respond fast enough during transients.

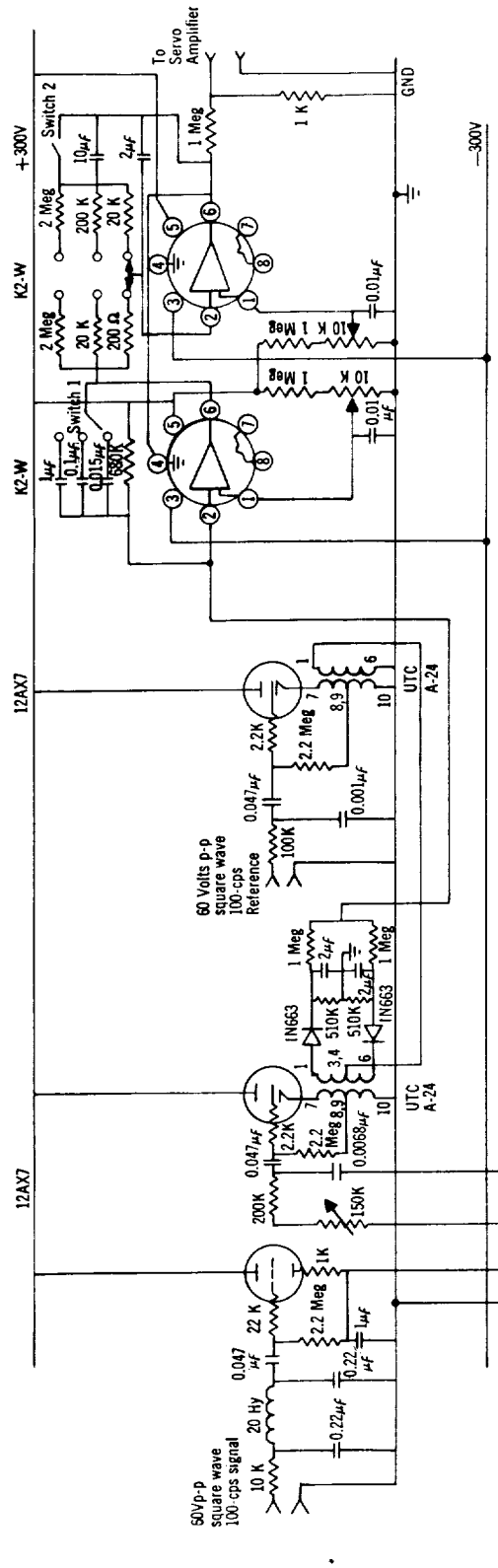

Figure 7—Schematic of filter, phase shifter, phase detector, and operational amplifier for phase-locked phase filter

PERFORMANCE TESTING

Performance tests were run at the three bandwidths 0.03, 0.3, and 3 cps. Those at 3 cps were unsatisfactory because of the high gear ratio. Figure 8 shows some of the results of the tests at 0.03 cps. Record 1 shows a transit of a radio star (Cygnus A) over the Blossom Point, Maryland, Minitrack station; channel a is the output of the Minitrack phase meter and channel b is the same information from the filter described in this report. It is interesting to note the sharp crossovers here as compared to other postdetection filtering techniques that have been used before in which the crossover is rounded. The signal is clear enough to be used for station calibration purposes. Record 2 shows a Minitrack system internal calibration with signal strengths from -100 to -145 dbm. At -140 dbm the phase noise of the system is ± 50 percent of a wavelength peak-to-peak (channel a) as compared to ± 1.5 percent of a wavelength when using the filter (channel b). Even at -145 db, where it is not possible to see any signal in the normal channel, the deviations on the filtered channel are less than ± 2.0 percent of a wavelength. Record 3 shows the response (channel a) of the system to a step-plus-ramp input (channel b) with a rate of 4.0 percent of a wavelength/second. Record 4 shows the system error (channel b) for the same type input, and also shows how the error is reduced to zero after a transient time slightly less than the theoretical 80 seconds. Records 5 and 6 show the response (channels a) and error (channels b) for a step input; the scale of 6b has been multiplied by 5 to show the error on a larger scale.

Figure 9 shows the performance of the system at the 0.3 cps bandwidth. Record 1 is a simulated noisy pass showing the acquisition and smoothing of the information; channel a is the output of the filter, and channel b the output of a normal Minitrack channel. Record 2 is a record of an actual satellite pass with a phase rate of 15 percent of a wavelength/second, channel a is the normal Minitrack record and channel b the filtered output. The acquisition transient was over before the satellite was in the main beam (the discontinuities in record are due to a change in paper speed). Notice that there is no phase shift throughout the pass. Record 3 shows the system response (channel a) to a ramp input (channel b). Record 4 shows the system error (channel b) for a ramp-plus-step input (channel a). Records 5 and 6 show the system response and error to a step input. All transients are over within the theoretical 8 seconds. Record 7 shows a Minitrack system calibration (channel a) with a variable signal strength from -100 to -145 dbm. At -140 dbm the noise deviations are reduced from ± 50 percent (channel a) to ± 6.0 percent (channel b) of a wavelength.

REFERENCES

1. Mengel, J. T., "Tracking the Earth Satellite, and Data Transmission, by Radio," *Proc. IRE* 44(6):755-760, June 1956

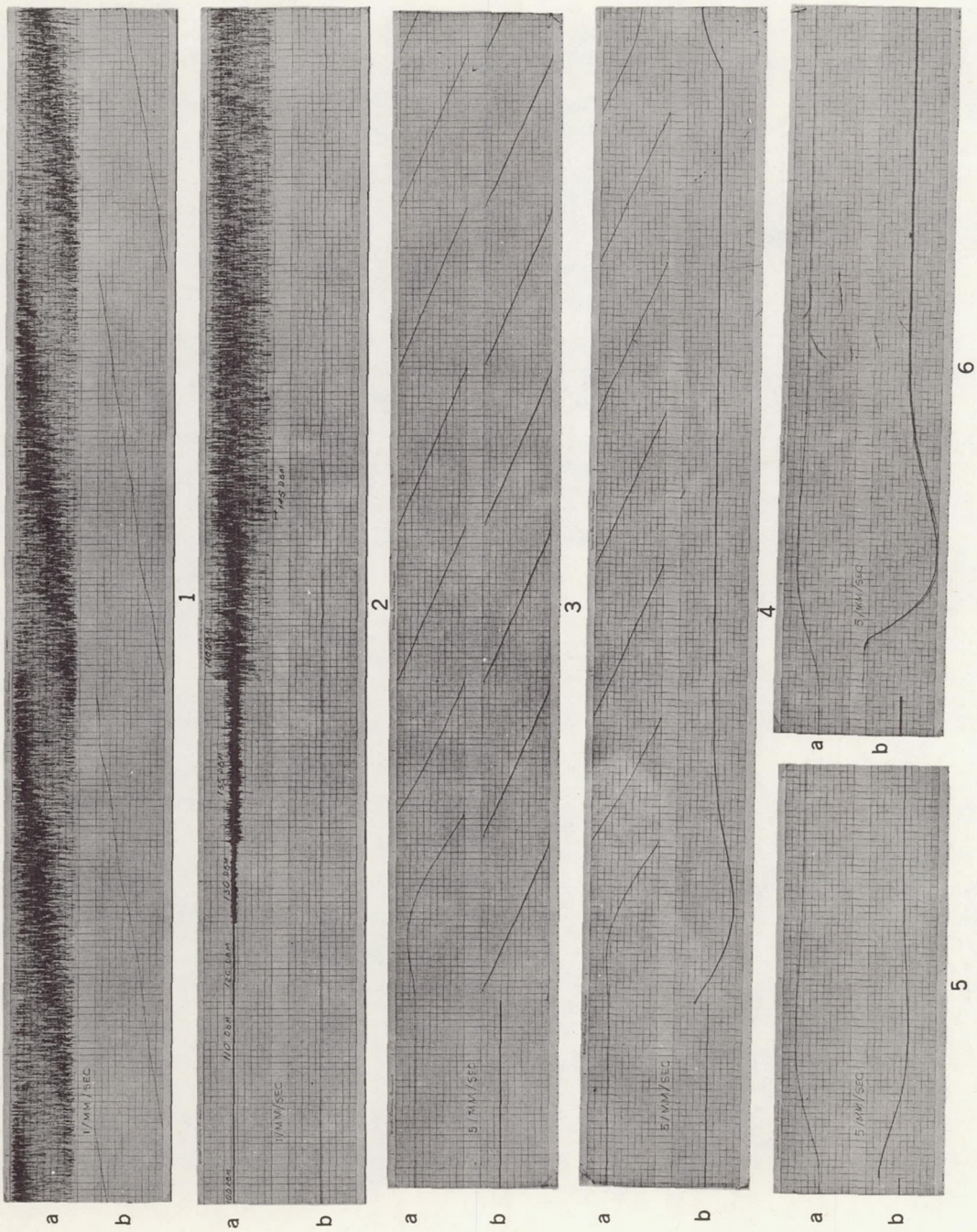

Figure 8—System performance at 0.03 cps bandwidth

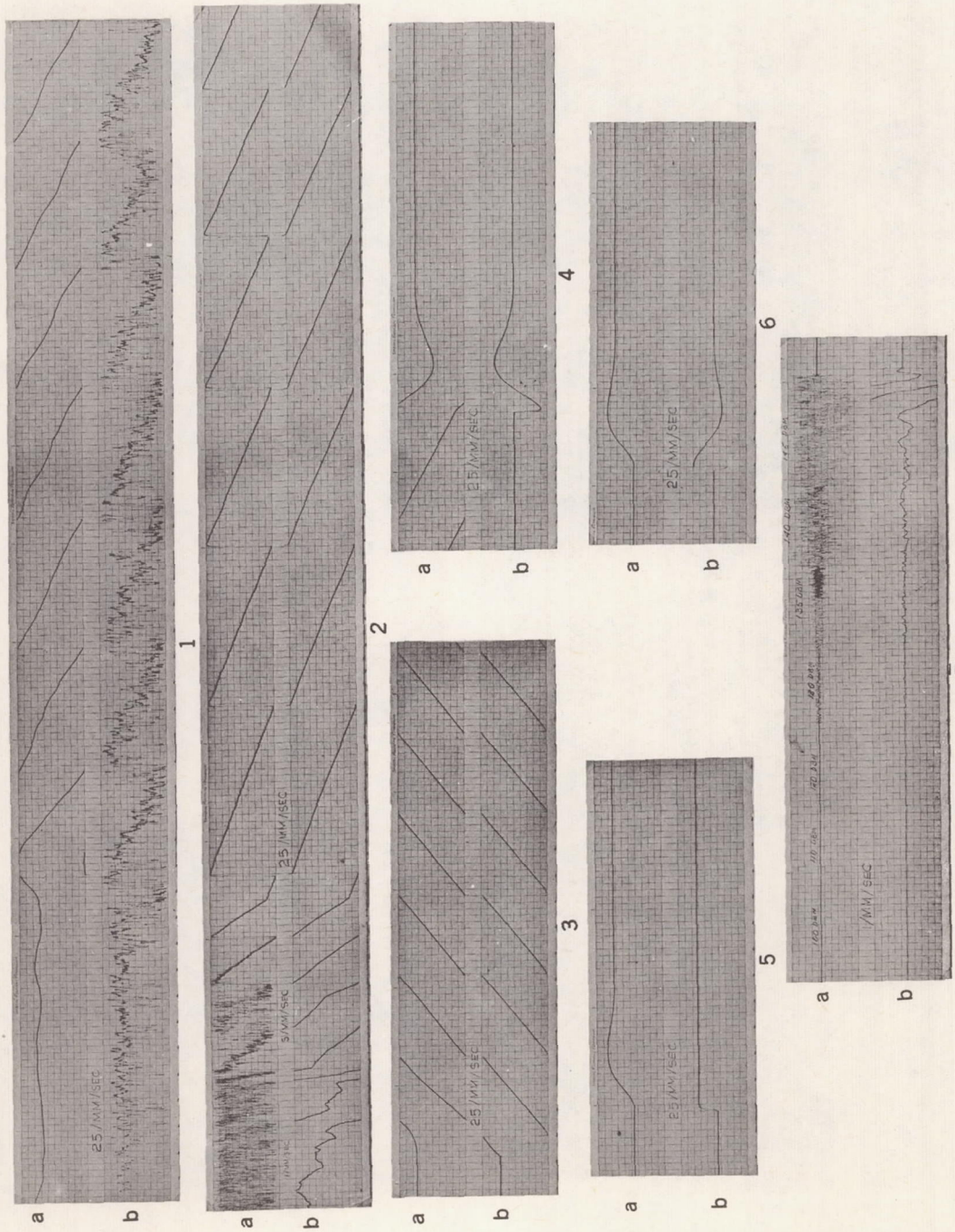

Figure 9—System performance at 0.3 cps bandwidth

2. Schroeder, C. A., Looney, C. H., Jr., and Carpenter, H. E., Jr., "Project Vanguard Report No. 18, Minitrack Report No. 1, Phase Measurement," U. S. Naval Research Lab. Report 4995, July 26, 1957

3. Schroeder, C. A., Looney, C. H., Jr., and Carpenter, H. E., Jr., "Tracking Orbits of Man-made Moons," *Electronics* 32(1):33-37, January 2, 1959

NASA-Langley, 1962 G-225